(33) B. M. Mattson, J. R. Heiman, and L. H. Pignolet, to be submitted for publication.
(34) A. M. Bond, A. R. Hendrickson, and R. L. Martin, *J. Am. Chem. Soc.*, **95**, 1449 (1973).
(35) L. H. Pignolet, G. S. Patterson, J. F. Weiher, and R. H. Holm, *Inorg. Chem.*, **13**, 1263 (1974).
(36) A. R. Hendrickson, R. L. Martin, and N. M. Rohde, *Inorg. Chem.*, **13**, 1933 (1974).
(37) F. A. Cotton, *Acc. Chem. Res.*, **2**, 240 (1969).
(38) The $[Fe(Me_2dtc)_3]^+$ cation has been characterized by electronic absorption, ^1H NMR, and ir spectroscopy.
(39) C. Oldham, *Prog. Inorg. Chem.*, **10**, 223 (1968).
(40) D. Coucouvanis, S. J. Lippard, and J. A. Zubieta, *Inorg. Chem.*, **9**, 2775 (1970).
(41) L. Ricard, P. Karagiannidis, and R. Weiss, *Inorg. Chem.*, **12**, 2179 (1973).
(42) R. Hesse, *Ark. Kemi*, **20**, 481 (1963).
(43) M. Monamico, G. Dessy, A. Mugnoli, A. Vaciago, and L. Zambonelli, *Acta Crystallogr.*, **19**, 885, 889 (1965).
(44) H. Hellawell and W. Hume-Rothery, *Philos. Mag.*, **45**, 797 (1954).
(45) M. J. Bennett, K. G. Caulton, and F. A. Cotton, *Inorg. Chem.*, **8** (1969); F. A. Cotton, *Chem. Soc. Rev.*, **4**, 27 (1975).
(46) R. Mason and A. I. M. Rae, *J. Chem. Soc. A*, 778 (1968).
(47) (a) R. Belford, M. I. Bruce, M. A. Cairns, M. Green, H. P. Taylor, and P. Woodward, *Chem. Commun.*, 1159 (1970); (b) M. R. Churchill, K. Gold, and P. H. Bird, *Inorg. Chem.*, **8**, 1956 (1969); (c) M. R. Churchill and J. Wormald, *J. Am. Chem. Soc.*, **93**, 5670 (1971); (d) R. Mason and W. R. Robinson, *Chem. Commun.*, 468 (1968); (e) P. J. Roberts and J. Trotter, *J. Chem. Soc. A*, 3246 (1970); (f) D. B. W. Yawney and R. J. Doedens, *Inorg. Chem.*, **11**, 838 (1972); (g) M. R. Churchill and J. Wormald, *ibid.*, **12**, 191 (1973).
(48) L. H. Pignolet, *Inorg. Chem.*, **13**, 2051 (1974).
(49) D. Coucouvanis and S. J. Lippard, *J. Am. Chem. Soc.*, **91**, 307 (1969).
(50) R. Eisenberg, *Prog. Inorg. Chem.*, **12**, 295 (1970).
(51) H. Abrahamson, J. R. Heiman, and L. H. Pignolet, *Inorg. Chem.*, **14**, 2070 (1975), and references cited therein.
(52) L. F. Dahl, E. R. de Gil, and R. D. Feltham, *J. Am. Chem. Soc.*, **91**, 1653 (1969).
(53) F. A. Cotton, *Rev. Pure Appl. Chem.*, **17**, 25 (1967).

Contribution from the Department of Chemistry,
University of Alberta, Edmonton, Alberta, Canada T6G 2E1

Bis(dimethyldithioarsinato)oxovanadium(IV) and Its Complexes with Lewis Bases

E. D. DAY and R. E. D. McCLUNG*

Received September 3, 1975 AIC506553

The preparation and physical characteristics of bis(dimethyldithioarsinato)oxovanadium(IV) and the results of an ESR investigation of the interaction of this complex with Lewis bases in toluene solutions are described. Thermogravimetric, infrared, mass spectral, and magnetic susceptibility data for the complex are given, as well as thermogravimetric and infrared data for a green solid, $OV[S_2As(CH_3)_2]_2 \cdot x$py with $x \simeq 4$, obtained by solvent removal from a pyridine solution of the complex. The ESR results indicate that the behavior of the dithioarsinate complex with Lewis bases is similar to that of the corresponding dithiophosphinate complex in that the chelating ligands sequentially become monodentate with a Lewis base molecule occupying the coordination site from which the sulfur atom is displaced. The equilibrium constants and thermodynamic parameters for the ligand displacement equilibria are reported.

Introduction

In a previous electron spin resonance (ESR) study in this laboratory,[1] which was substantiated independently,[2,3] the coordination of Lewis bases to vanadyl dithiophosphinate complexes was illucidated. On the basis of ESR, optical, and infrared measurements on the complexes $OV(S_2PX_2)_2$, X = CH_3,[1] C_6H_5,[1] and OC_2H_5,[1-3] in solutions containing various concentrations of the Lewis bases pyridine,[1-3] hexamethylphosphoramide,[1] or dimethylformamide,[1] it was concluded that the equilibria 1 and 2, where Y is phosphorus and L is a Lewis

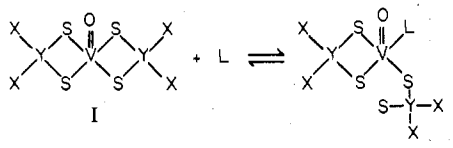

I + L ⇌ II (1)

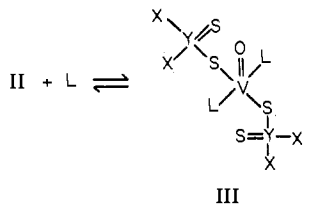

II + L ⇌ III (2)

base, are present in these solutions. It was concluded[1] on the basis of infrared evidence that species II may exist in a form in which the sixth coordination site of the vanadium atom trans to the vanadyl oxygen is vacant or in a form where the sulfur atom of the dithiophosphinate, which is displaced by the ligand L, occupies this coordination site. Furthermore, the relative orientation of the monodentate ligands in species III was not ascertained. At very high concentrations of Lewis base, the dithiophosphinate ligands are completely displaced from the first coordination sphere of the vanadyl ion.[1] The enthalpy of reaction 1 was determined from the relative intensities of the ESR[1,3] and optical absorptions[3] of species I and II.

The chelate displacement equilibria described above are in sharp contrast with the addition equilibria which have been suggested in the interaction of Lewis bases with vanadyl acetylacetonate,[4] eq 3 and 4. Experimental measurements

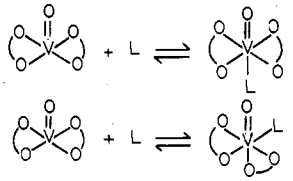

(3)

(4)

of the interactions of other vanadyl complexes with Lewis bases have generally been interpreted in terms of reaction 3.[5]

The transition metal complexes with dithioarsinate ligands[6-9] form a series of complexes which parallels the series of dithiophosphinate complexes.[1-3,10-12] The existing body of published work indicates that substitution of an arsenic atom for a phosphorus atom in what is effectively the second coordination sphere of the metal ion does not produce significant changes in the electronic properties of the metal complexes. The preparation and electronic and ESR spectra of bis(dimethyldithioarsinato)oxovanadium(IV) were reported[9,10] while the present work was in progress. The ESR spectra of $OV[S_2As(CH_3)_2]_2$ are different from those of $OV[S_2P(CH_3)_2]_2$[1-3,11,12] since ^{75}As has spin $^3/_2$ while ^{31}P has spin $^1/_2$. However, the magnitude of the isotropic ^{75}As hyperfine coupling indicates that the distribution of unpaired electron density in $OV[S_2As(CH_3)_2]_2$ is similar to that in $OV[S_2P(CH_3)_2]_2$. The isolation of the bis(pyridine) adduct of

* To whom correspondence should be addressed at the Physics Laboratory, University of Kent, Canterbury, Kent, England.

Table I

Compd	% C		% H		% S		% N	
	Calcd	Found	Calcd	Found	Calcd	Found	Calcd	Found
$OV[S_2As(CH_3)_2]_2$	11.86	11.85	2.99	2.82	31.65	31.87		
$NaS_2As(CH_3)_2 \cdot 2H_2O$	10.53	10.88	4.42	4.26	28.11	27.93		
$OV[S_2As(CH_3)_2]_2 \cdot x$py	39.95[a]	38.06–39.68[b]	4.47[a]	4.43–4.85[b]			7.76[a]	7.05–7.68[b]

[a] Calculated for $x = 4$. [b] Values varied from sample to sample. Observed range of values is given.

$Ni[S_2As(CH_3)_2]_2$ has been reported,[7,8] and the variation in the electronic spectrum of $Ni[S_2As(CH_3)_2]_2$ with solvent donor strength has been discussed,[7] but no reports of the interaction of Lewis bases with $OV[S_2As(CH_3)_2]_2$ have appeared.

In this paper, we present the results of physical measurements on $OV[S_2As(CH_3)_2]_2$ and the solid, $OV[S_2As(CH_3)_2]_2 \cdot x$py, obtained by solvent removal from a pyridine solution of $OV[S_2As(CH_3)_2]_2$. The results of ESR and infrared studies of $OV[S_2As(CH_3)_2]_2$ in inert solvents and in solutions containing different concentrations of Lewis bases are also reported and are interpreted in terms of equilibria 1–4.

Experimental Section

Instrumentation. Infrared spectra were obtained on Perkin-Elmer 421 and Beckman IR-11 instruments, using CsBr plates. Mass spectra were obtained by means of the direct-probe sample insertion system of the AEI MS9 mass spectrometer operating at 70 eV. Magnetic susceptibilities were measured by the Faraday technique as described elsewhere.[11] Thermogravimetric analyses were carried out under rotary oil pump vacuum using the Du Pont Model 900 differential thermal analyzer equipped with Model 950 thermogravimetric analyzer attachment. The ESR spectra were obtained with a Varian V-4502 spectrometer system described previously.[1] g values were measured relative to Fremy's salt ($g = 2.00550$),[13] and the magnetic field was calibrated using an Alpha Model 3093 digital NMR gaussmeter. Analyses (C, H, S, and N) were performed by the microanalytical service of the University of Alberta. Analytical data are given in Table I.

Syntheses. (a) $NaS_2As(CH_3)_2 \cdot 2H_2O$ was prepared by passing H_2S(g) through a hot ethanolic solution of $NaO_2As(CH_3)_2$ as described.[6]

(b) $OV[S_2As(CH_3)_2]_2$. A mixture of $OVSO_4 \cdot 2H_2O$ (5 mmol) and $NaS_2As(CH_3)_2 \cdot 2H_2O$ (10 mmol) was stirred in 25 ml of methanol in a stoppered flask for 2 hr. The methanol was removed under vacuum, and the solid extracted with 25 ml of CH_2Cl_2 in a Soxhlet extractor for 6 hr. When extraction was complete, 25 ml of 2-propanol was added to the deep blue CH_2Cl_2 solution and the volume reduced on a rotary evaporator over a hot water bath. The lustrous deep blue crystals were filtered off, were washed with 2-propanol and then diethyl ether, and were air-dried. The crystals were stored in closed vials (stench!) for periods of weeks without visible deterioration. The low solubility of the complex in organic solvents precluded a solution molecular weight determination. Mass spectrometric analysis gave m/e 404.7635 (calcd 404.7643).

(c) $OV[S_2As(CH_3)_2]_2 \cdot x$py. Pyridine, dried over P_2O_5, was condensed onto a sample of $OV[S_2As(CH_3)_2]_2$ in a conventional vacuum system and produced an emerald green solution. On removal of the excess pyridine under vacuum, an emerald green solid formed. Elemental analysis (Table I) indicated that the number of pyridine moieties associated with each $OV[S_2As(CH_3)_2]_2$ unit was close to 4 but varied from sample to sample.

(d) $(CH_3)_2As(S)SAs(CH_3)_2$ was prepared by the method reported by Zingaro et al.[14]

Preparation of ESR Samples. To ensure the exclusion of oxygen and water contamination from the toluene solutions of $OV[S_2As(CH_3)_2]_2$ and pyridine for the ESR studies, all samples were prepared with the apparatus shown in Figure 1. The steps in the sample preparation are described briefly. (1) A weighed sample (~10 mg) of $OV[S_2As(CH_3)_2]_2$ was introduced into the apparatus with stopcock no. 1 removed. The apparatus was closed, evacuated, and weighed. (2) The approximate volume of pyridine desired was condensed into the apparatus from a degassed reservoir maintained over P_2O_5, and the apparatus was reweighed to determine the precise quantity of pyridine added. (3) Sufficient toluene to make up 5 ml of solution was condensed into the apparatus from a degassed reservoir maintained over P_2O_5, and the apparatus was reweighed to determine the precise quantity of toluene added. (4) With stopcock no. 1 tightly closed, a Pyrex sample tube (3–4 mm o.d.) sealed to a standard taper joint was connected below stopcock no. 3, evacuated, degassed, and tested for leaks. (5) With stopcock no. 2 tightly closed and stopcocks no. 1 and 3 open, the apparatus was tipped so that sufficient solution entered the sample tube. Stopcock 1 was closed, the sample tube was immersed in liquid nitrogen, stopcock no. 2 was opened to the vacuum line, and the sample tube was sealed off with a torch.

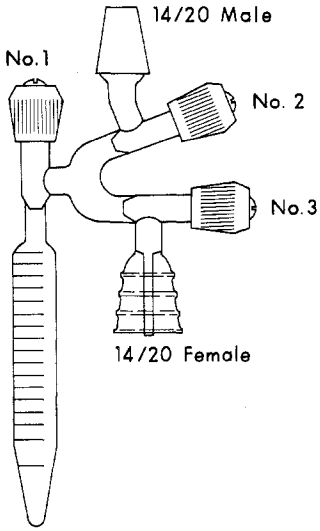

Figure 1. Apparatus for preparation of ESR samples.

Steps 4 and 5 were repeated to obtain replicate samples. All samples were stored in liquid nitrogen prior to the ESR study.

The solutions of $OV[S_2As(CH_3)_2]$ in neat toluene were prepared by decanting the saturated solution from undissolved crystalline complex because the solubility in toluene is very low. For measurement of the ESR spectra of $OV[S_2As(CH_3)_2]$ in solid toluene solutions, a special sample tube was constructed with a narrow portion which protruded below the microwave cavity when the tube was placed in the variable-temperature insert of the ESR spectrometer. This narrow portion accomodated a single crystal of the solid complex, with toluene solution above it. In order to obtain solid solution with sufficient concentrations of $OV[S_2As(CH_3)_2]_2$ to produce ESR spectra with a satisfactory signal-to-noise ratio, it was necessary to heat the sample tube containing the single crystal and toluene solution to 90 °C and then plunge the tube into liquid nitrogen.

Results

A. Characterization of $OV[S_2As(CH_3)_2]_2$ and $OV[S_2As(CH_3)_2]_2 \cdot x$py. In most respects, $OV[S_2As(CH_3)_2]_2$ resembles its phosphorus analogue, $OV[S_2P(CH_3)_2]_2$, except for the vile odor and very low solubility of $OV[S_2As(CH_3)_2]_2$ in noncoordinating solvents. $OV[S_2As(CH_3)_2]_2$ was found to decompose on heating under vacuum before sublimation occurred. The durability of the complex has been reported previously.[9] The stability of solutions of $OV[S_2As(CH_3)_2]_2$ can be prolonged significantly by rigorous degassing and dehydration of solvents and storage vessels. Solutions containing dimethylformamide (DMF) were less stable than solutions containing pyridine, but both eventually decompose to form a black residue when the solutions are kept at room temperature for extended periods. Decomposition occurs more rapidly at higher temperatures and reproducible ESR mea-

Table II. Mass Spectrum of $OV[S_2As(CH_3)_2]_2$[a]

Assignment	Rel intens	*m/e*, amu	Assignment	Rel intens	*m/e*, amu
$OVS_4As_2(CH_3)_4^+$	100	404.7635 (calcd 404.7643)	$OVS_4As(CH_3)_2^+$	15	300
$OVS_4As_2(CH_3)_3^+$	11	390	$OVS_3As(CH_3)^+$	8	253
$OVS_4As_2(CH_3)_2^+$	21	375	$OVS_2As(CH_3)_2^+$	22	236
$VS_2As_2(CH_3)_4^+$	15	325	OVS_2As^+	16	206
			OVS_4^+	8	195

[a] Source temperature 150 °C.

Table III. Isotropic Magnetic Paramaters[a] for $OV[S_2As(CH_3)_2]_2$ and Its Pyridine Derivatives in Pyridine–Toluene Solutions

Species	25 °C			60 °C			90 °C		
	g_0	a^V	a^{As}	g_0	a^V	a^{As}	g_0	a^V	a^{As}
I	1.9718	92.8	43.5	1.9714	93.0	43.0	1.9710	93.3	43.1
II	1.9729	93.6	31.9	1.9723	93.6	31.7	1.9715	93.7	31.7
III	1.9743	93.5		1.9736	93.7		1.9730	94.2	

[a] Hyperfine splittings are in gauss. Estimated errors are ±0.5 G for hyperfine splittings and ±0.0005 for *g* values.

surements could not be obtained at temperatures above 90 °C.

Mass Spectrum of $OV[S_2As(CH_3)_2]_2$. The assignment and relative intensities of the mass spectral peaks corresponding to metal-containing ions are given in Table II. The cracking pattern of $OV[S_2As(CH_3)_2]_2$ is very different from that of $OV[S_2P(CH_3)_2]_2$,[11] but the parent peaks are dominant features of the mass spectra of both complexes. It should be pointed out that the odor associated with $OV[S_2As(CH_3)_2]_2$ and its fragments contaminated the mass spectrometer for several days.

Magnetic Susceptibilities. The magnetic susceptibility of $OV[S_2As(CH_3)_2]_2$ was measured over the temperature range 88–313 K. The magnetic susceptibility data show a Curie–Weiss temperature dependence and correspond to an effective magnetic moment of 1.725 BM, which compares well with the "spin-only" value of 1.732 BM, with the value 1.708 BM derived from $3^{1/2}g/2$ using the solution *g* value from ESR measurements, and with the value 1.72 BM reported[11] for $OV[S_2P(CH_3)_2]_2$.

Measurements of the room-temperature magnetic susceptibility of $OV[S_2As(CH_3)_2]_2 \cdot x$py gave a net diamagnetism which is consistent with a metal complex, with a single unpaired electron, enveloped by a large number of diamagnetic groups. The imprecise composition of $OV[S_2As(CH_3)_2]_2 \cdot x$py precluded more careful susceptibility studies.

Thermogravimetric Measurements. The thermogram of $OV[S_2As(CH_3)_2]_2$ showed that decomposition with evolution of volatile products occurs near 217 °C. The weight loss (found 76.1%) corresponded to the loss of $(CH_3)_4As_2S_3$ (calculated 75.6%), implying a residue of OVS.

Thermogravimetric analysis of $OV[S_2As(CH_3)_2]_2 \cdot x$py showed that pyridine loss began at 56 °C and occurred continuously up to about 150 °C. There was no indication of stepwise removal of pyridine from the complex. The weight loss varied slightly from sample to sample but indicated a stoichiometry of approximately four pyridine molecules to each $OV[S_2As(CH_3)_2]_2$ molecule. The infrared spectrum of the solid residue after the removal of pyridine was identical with that of $OV[S_2As(CH_3)_2]_2$.

B. ESR Measurements. The ESR spectra of a solution of $OV[S_2As(CH_3)_2]_2$ in toluene (saturated solution at 25 °C) at 25, 60, and 90 °C are shown in Figure 2 and are similar to those reported by other workers.[9,10] These liquid solution spectra consist of eight lines due to interaction of the unpaired electron with the ^{51}V nuclear spin ($I = 7/2$, hyperfine splitting a^V); each of these eight lines is further split into a 1:2:3:4:3:2:1 septet of lines due to interaction of the electron with two equivalent ^{75}As nuclei ($I = 3/2$, hyperfine splittings a^{As}). Many of the 56 possible lines are not resolved even at 90 °C because a^{As} is approximately half as large as a^V. It is apparent from the variations in the intensities of the lines that the widths

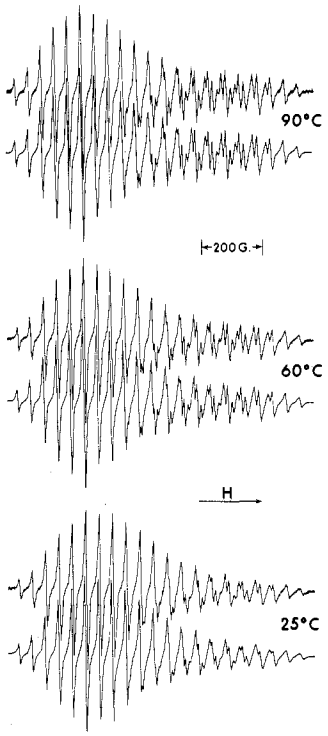

Figure 2. ESR spectra of $OV[S_2As(CH_3)_2]_2$ in toluene (saturated solution at 25 °C) at temperatures indicated. The experimental spectrum is shown above the computed spectrum in each case.

of the different hyperfine components vary with the ^{51}V nuclear spin quantum number as is common in vanadyl complexes.[15] Since the overlapping of lines and the variation in their widths prevent direct determination of the hyperfine splittings a^V and a^{As} from the spectra, the observed spectra were compared with those synthesized by superposition of Lorentzian line shapes on a digital computer.[16] The computed spectra which agreed best with the observed ones are included in Figure 2.

The values of the hyperfine parameters a^V and a^{As} and the isotropic *g* value, g_0, determined from the toluene solutions are given in Table III. The temperature dependence of these magnetic parameters is similar to that observed in the acetylacetonate[17] and dithiophosphinate[1] complexes and suggests that the molecular structure does not change with temperature.

The ESR spectrum of $OV[S_2As(CH_3)_2]_2$ in solid toluene solution at −163 °C is shown in Figure 3. This spectrum can be interpreted in terms of an axially symmetric spin Hamiltonian[1] because of the small differences to be expected

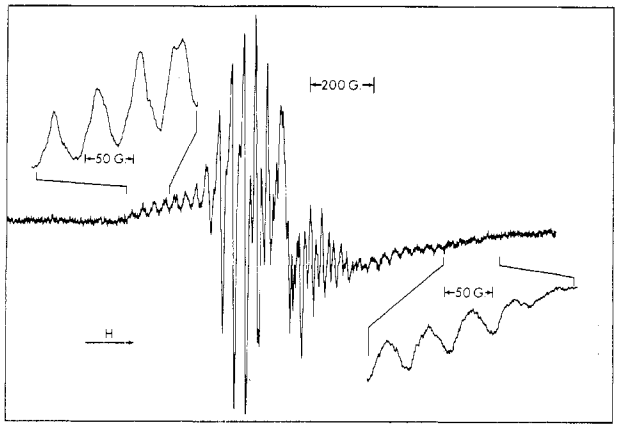

Figure 3. ESR spectrum of $OV[S_2As(CH_3)_2]_2$ in solid toluene at −163°C. The inserts show the parallel regions of the spectrum on an expanded scale.

Table IV. Anisotropic Magnetic Parameters[a] for $OV[S_2As(CH_3)_2]_2$ and Its Pyridine Derivatives in Solid Pyridine–Toluene Solutions at −163 °C

Species	$g_\parallel$	$g_\perp$	$a^V_\parallel$	$a^V_\perp$	$a^{As}_\parallel$	$a^{As}_\perp$
I	1.934	1.991[b]	160	59[b]	44	43[b]
III	1.958	1.979	167	58		

[a] Hyperfine splittings are in gauss. Estimated errors are ±0.002 in g values and ±1 G in splittings. [b] Values of parameters for the directions perpendicular to the V–O axis were determined from values of parallel parameters and from isotropic parameters at 25 °C with eq 5 and 6.

in the two directions perpendicular to the V–O axis. Since there is considerable overlapping of lines in the perpendicular (central) part of the spectrum, only $g\parallel$, $a^V\parallel$, and $a^{As}\parallel$ could be determined directly from the spectrum. The values of the corresponding parameters for the perpendicular directions were calculated from the isotropic and parallel values using the relations

$$g_\perp = (3g_0 - g_\parallel)/2 \quad (5)$$

$$a_\perp = (3a - a_\parallel)/2 \quad (6)$$

The values of the anisotropic magnetic parameters which describe the glass spectrum are given in Table IV. Clearly, the ^{57}As hyperfine interactions are shown to be isotropic within the experimental uncertainties. This isotropy of hyperfine interactions for nuclei in the second coordination sphere also occurs in the dithiophosphinate complexes.[1]

The appearance of the ESR spectra of $OV[S_2As(CH_3)_2]_2$ is changed dramatically when pyridine is added to the toluene solution. The spectra indicate that these solutions contain vanadyl species in which the unpaired electron interacts with two (species I), one (species II), and zero (species III) ^{75}As nuclei just as solutions of the vanadyl dithiophosphinates contain vanadyl species where the unpaired electron interacts with two, one, and zero ^{31}P nuclei. In the dithioarsinate case, each of the three species makes significant contributions to the ESR spectra over wide ranges of concentration of pyridine and temperature while the spectra of the dithiophosphinates contained important contributions from only two of the three species under most conditions.[1]

The ESR spectra of 10^{-3} M solutions of $OV[S_2As(CH_3)_2]_2$ in pyridine–toluene solvents with different pyridine concentrations at various temperatures are shown in Figure 4. The mole fractions of the three vanadyl species, which were obtained by fitting the observed ESR spectra with computed ones,[16] are summarized in Table V. Clearly the simulation of each spectrum requires estimates of the mole fractions of each species and the g factor, hyperfine splittings, and line

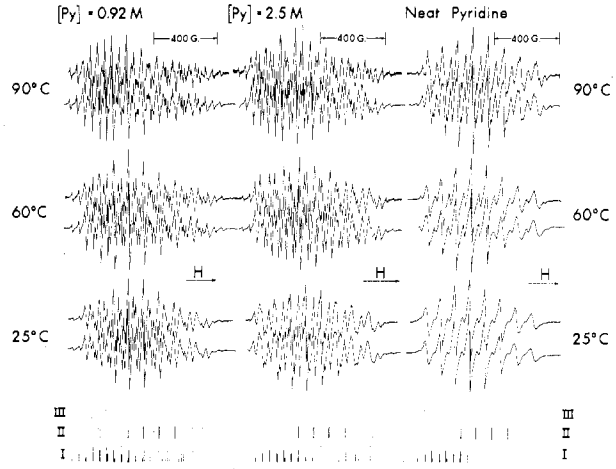

Figure 4. ESR spectra of $OV[S_2As(CH_3)_2]_2$ and its pyridine derivatives in pyridine–toluene solutions at various temperatures. The calculated spectra which agreed best with the observed ones are shown below the observed spectra, and stick spectra for the three vanadyl species are given at the bottom of the figure.

Table V. Mole Fractions of the Vanadyl Dithioarsinate Species in Toluene–Pyridine Solutions[a]

Temp, °C	[py], M	x_I	x_{II}	x_{III}
22	0.31	0.32	0.59	0.09
23	0.53	0.20	0.64	0.16
23	0.96	0.14	0.59	0.27
27	0.92	0.14	0.61	0.25
26	2.45	0.06	0.39	0.55
25	3.37	0.10	0.30	0.60
26	4.94		0.34	0.66
24	Neat		0.15	0.85
50	0.92	0.25	0.60	0.15
60	0.92	0.30	0.56	0.14
60	2.45	0.12	0.54	0.34
60	3.37	0.10	0.48	0.42
60	4.94	0.09	0.41	0.50
60	Neat		0.20	0.80
90	0.92	0.52	0.38	0.10
90	2.45	0.23	0.51	0.26
90	4.94	0.20	0.48	0.32
90	Neat	0.08	0.27	0.65

[a] Errors in the mole fractions are estimated to be ±10% of the fractions quoted.

widths for each. As described in the Appendix, the initial estimates were refined until satisfactory agreement between computed and observed spectra, as determined by visual comparison and by the sum of squared residuals, was obtained. Satisfactory simulations were obtained by treating the ^{51}V and ^{75}As hyperfine interactions to second order[1,17] and by requiring the widths of the different hyperfine lines, with the same value of the ^{51}V nuclear spin quantum number but different values of the ^{75}As nuclear spin quantum number, to be equal for a given vanadyl species. In order to minimize ambiguities in these multiparameter fits of the observed spectra, the final simulations of the spectra of $OV[S_2As(CH_3)_2]_2$ in solutions with different pyridine concentrations, at a given temperature, employed the same set of g values, hyperfine splittings, and line widths and refined only the mole fractions of the three vanadyl species. It is likely that some systematic errors were incurred by this procedure because the line widths and, less significantly, the hyperfine splittings and g factors are expected to vary with solvent composition. However, the variations in the line widths for each vanadyl species are expected to be comparable so that any errors incurred are probably less than those produced by convergence to false or local minima in a multiparameter fit. In no case did the mole fractions in the free multiparameter fit differ from those obtained in the final

simulation by more than the estimated error of ±10% of the values quoted in Table V. The magnetic parameters which characterize species II and III were obtained from the comparison of observed and computed spectra and are given in Table III together with the parameters for species I which were determined from the ESR spectra of $OV[S_2As(CH_3)_2]_2$ in toluene.

The ESR spectra of the solid solutions of $OV[S_2As(CH_3)_2]_2$ in toluene containing pyridine did not vary with pyridine concentration. In all cases, the solid solutions were green and gave ESR spectra characteristic of a vanadyl species in which the unpaired electron interacts only with the ^{51}V nucleus (species III). The magnetic parameters for both parallel and perpendicular directions were obtained directly from the spectra, without recourse to the isotropic values obtained from liquid spectra and eq 5 and 6, and are given in Table IV. The isotropic magnetic parameters for species III (Table III) are consistent with the anisotropic parameters in Table IV.

Qualitative examination of the ESR spectra of $OV[S_2As(CH_3)_2]_2$ in toluene solutions containing hexamethylphosphoramide or dimethylformamide indicated the presence of the three vanadyl species in these solutions. No detailed studies of these systems were made since they exhibited less thermal stability than solutions containing pyridine.

Infrared Measurements. In order to obtain information about the structures of vanadyl dithioarsinate–pyridine adducts II and III, we have made infrared measurements on anhydrous $NaS_2As(CH_3)_2$, $(CH_3)_2As(S)SAs(CH_3)$, and $OV[S_2As(CH_3)_2]_2$ in CS_2–pyridine and in neat pyridine.

The V–O, VS_4, and AsS_2 vibrations should reflect changes in the bonding in vanadyl dithioarsinate when it interacts with Lewis bases. The V–O stretch shifts from 985 cm^{-1} in solid $OV[S_2As(CH_3)_2]_2$ to 960 cm^{-1} in $OV[S_2As(CH_3)_2]_2 \cdot x$py solid and shows peaks at 985, 970, and 940 cm^{-1} in a saturated solution of $OV[S_2As(CH_3)_2]_2$ in CS_2 containing 0.7 M pyridine. The latter medium was chosen because our ESR data indicated that species II has its maximum concentration in toluene containing 0.7 M pyridine at room temperature. Since pyridine itself has absorptions in this spectral region (991 cm^{-1}), one can only conclude that the infrared absorptions in the V–O stretch region are compatible with $OV[S_2As(CH_3)_2]_2$–pyridine complexes where the axial position is occupied by either a pyridine or a dithioarsinate ligand in that the shifts in V–O stretching frequency on addition of pyridine are comparable to those observed in the vanadyl acetylacetonate–pyridine complexes.[4]

The AsS_2 stretching frequencies occur in the region 350–480 cm^{-1} wherein pyridine and CS_2 have absorptions only near 400 cm^{-1}. The absorptions for the $OV[S_2As(CH_3)_2]_2$ and $OV[S_2As(CH_3)_2]_2 \cdot x$py solids and the solutions of $OV[S_2As(CH_3)_2]_2$ in pyridine and in CS_2 containing 0.7 M pyridine are compared with the absorptions for related dithioarsinate compounds in Table VI. The shift of ν_{asym} to higher frequency in the $OV[S_2As(CH_3)_2]_2$ systems containing pyridine indicates that asymmetric binding of the dithioarsinate ligand does occur but does not allow us to decide whether the sulfur atom which has been displaced by a pyridine molecule has migrated to the axial coordination position or whether it is bonded only to the arsenic atom in the As=S form.

Table VI. Frequencies of AsS_2 Stretching Modes in Dimethyldithioarsinate Compounds

Compd	Medium	Bonding	ν_{asym}, cm^{-1}	ν_{sym}, cm^{-1}
$NaS_2As(CH_3)_2$	Nujol mull	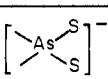	466 s	427 m, 418 m
$(CH_3)_2As(S)SAs(CH_3)_2$	Nujol mull	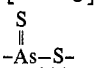	480 s	391 s, 357 s
$OV[S_2As(CH_3)_2]_2$	Nujol mull	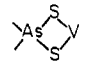	466 s	440 s
$OV[S_2As(CH_3)_2]_2 \cdot x$py	Nujol mull	?	478 s	455 s, 418 m
$OV[S_2As(CH_3)_2]_2$	0.7 M py–CS_2	?	480 w, sh, 475 w	445 w
$OV[S_2As(CH_3)_2]_2$	Pyridine	?	488 m	440 m

Discussion

Equilibria between Different Vanadyl Species. The ESR results presented in the previous section indicate that three dominant vanadyl species are present in toluene solutions of $OV[S_2As(CH_3)_2]_2$ containing Lewis bases in agreement with previous studies[1-3] of the analogous dithiophosphinate system. Unfortunately the infrared measurements offer no further insight into the structures of the $OV[S_2As(CH_3)_2]_2$–pyridine complexes (species II and III) than can be inferred from our infrared studies[1] of the $OV[S_2P(C_6H_5)_2]_2$–pyridine complexes. The equilibria present in toluene solutions of $OV[S_2As(CH_3)_2]_2$ and pyridine are undoubtedly represented by eq 1 and 2 with Y = As, X = CH_3, and L = py, and the structures of species II and III given above are consistent with all of our data.

We have investigated the possibilities

$$I + l\text{py} \rightleftharpoons II \quad (7)$$

$$II + l'\text{py} \rightleftharpoons III \quad (8)$$

with l and l' different from unity, but the mole fraction data in Table V were found to be most consistent with $l = l' = 1$. The equilibrium constants K_1 and K_2 for reactions 1 and 2 were determined from the mole fraction data in Table V and the enthalpies and entropies of reaction were determined. It must be pointed out that the variation in the polarities of the solvents from 0.3 M pyridine–toluene to 4.94 M pyridine–toluene is rather large so that the enthalpies and entropies of reaction determined from these data are necessarily approximate since the variation in the equilibrium constants K_1 and K_2 determined at different pyridine concentrations at a given temperature is considerable. In several cases, the precision of either K_1 or K_2 was low because the mole fraction of either species III or I was low. We have therefore fit the mole fraction data to the equations

$$\ln (x_{II}/x_I[\text{py}]) = \Delta H_1^\circ/RT + \Delta S_1^\circ/R \quad (9)$$

$$\ln (x_{III}/x_{II}[\text{py}]) = \Delta H_2^\circ/RT + \Delta S_2^\circ/R \quad (10)$$

using weights $x_I x_{II}$ and $x_{II} x_{III}$, respectively, in the least-squares procedure. The values of the enthalpies and entropies of reaction and the equilibrium constants at 25 °C are compared with those available for $OV[S_2PX_2]_2$–pyridine equilibria in Table VII. The only available datum on equilibrium 2 for comparison with this work is the value K_2 = 3.1 l./mol at −45 °C for $OV[S_2P(CH_3)_2]_2$–pyridine in CS_2.[1] Extrapolation of our data for $OV[S_2As(CH_3)_2]_2$–pyridine in toluene gives K_2 = 2.5 l./mol at −45 °C.

It is clear from the data in Table VII that reaction 1 is somewhat less exothermic for $OV[S_2As(CH_3)_2]_2$ than for $OV[S_2P(CH_3)_2]_2$. Reaction 2 is found to be less exothermic than reaction 1 for the $OV[S_2As(CH_3)_2]_2$ system and this must apply for the $OV[S_2P(CH_3)_2]_2$–pyridine system also since the enthalpy of reaction 1 for the $OV[S_2P(CH_3)_2]_2$ system must be greater than −6 kcal/mol in order to explain the observed value of K_1 at −45 °C and the apparent absence of species III in solutions at 25 °C.[1,18] Thus we can conclude that the complex formation reactions 1 and 2 are less exothermic for the dithioarsinate complex than for the dithiophosphinate complex.

The formation of the green solid $OV[S_2As(CH_3)_2]_2 \cdot x$py, with $x \simeq 4$, by removal of pyridine from a pyridine solution

Table VII. Enthalpies and Entropies of Reaction and Equilibrium Constants at 298 K for the $OV[S_2As(CH_3)_2]_2$-Pyridine and Related Equilibria

	Complex-ligand (solvent)			
	$OV[S_2As(CH_3)_2]_2$-py (toluene)	$OV[S_2P(CH_3)_2]_2$-py (CS_2)	$OV[S_2P(C_6H_5)_2]_2$-py (CS_2)	$OV[S_2P(OC_2H_5)_2]_2$-py (toluene)
ΔH_1°, kcal/mol	−5.8 ± 0.5	−9.3 ± 0.2[a]	−7.7 ± 0.4[a]	−11.5[b]
ΔS_1°, cal/(K mol)	−16 ± 2	−25[a]	−19[a]	−28.5[b]
K_1^{298K}, l./mol	5.2 ± 0.5	23[a]	31[a]	65[b]
ΔH_2°, kcal/mol	−3.2 ± 0.2			
ΔS_2°, cal/(K mol)	−12 ± 1			
K_2^{298K}, l./mol	0.51 ± 0.05			

[a] Reference 1. [b] Reference 3.

of the parent complex is difficult to reconcile with the isolation of $OV[S_2P(C_2H_5)_2]_2$·py by Hertel and Kuchen[19] but may reflect differences in substituents of the ligands. Since the ESR spectra of $OV[S_2As(CH_3)_2]_2$ in neat pyridine are consistent with the dominant species being $OV[S_2As(CH_3)_2]_2$·2py (species III), the formation of $OV[S_2As(CH_3)_2]_2$·$x$py with $x \simeq 4$ must occur during the crystallization process.

ESR Parameters. The magnetic parameters for $OV[S_2As(CH_3)_2]_2$ in toluene solutions (see Tables II and III) are in reasonable agreement with the values reported by McCormick et al.[9] for liquid solutions in benzene and chloroform. The small differences can be attributed to our thorough simulation of the ESR spectra while the previous workers did not include the variation in the line widths with the ^{51}V nuclear spin quantum number in their simulations.[9,10] However, McCormick et al.[9] were unable to observe ^{75}As splittings in the solid solutions as we have done (Figure 3). Their failure to observe these splittings indicates the presence of Lewis bases in their solvents since we never observed ^{75}As hyperfine interactions in solid spectra when pyridine, hexamethylphosphoramide, or dimethylformamide was present in the solutions, even at very low base concentrations.

The **g** tensor in $OV[S_2As(CH_3)_2]_2$ is found to be considerably more anisotropic than the **g** tensor in $OV[S_2P(CH_3)_2]_2$,[1] and the isotropic g value is slightly smaller in the dimethyldithioarsinate. The decrease from 94.8 to 92.8 G in the isotropic ^{51}V hyperfine splitting in going from $OV[S_2P(CH_3)_2]_2$ to $OV[S_2As(CH_3)_2]_2$ could be due to increased delocalization of the unpaired electron density onto the ligands, a conclusion consistent with the ^{75}As splitting as discussed below.

The mechanism of the hyperfine interaction between the ^{75}As nuclei in the dimethyldithioarsinate ligands with the unpaired electron on the vanadium atom is expected to be similar to that invoked in the dithiophosphinate complexes[1,9,12] and involves a σ interaction between the vanadium $d_{x^2-y^2}$ orbital and an appropriate linear combination of the two As–S σ-bonding orbitals. The hyperfine splittings can be related[9] to the coefficient C^{As}_{4s} of the arsenic 4s atomic orbital in the molecular orbital containing the unpaired electron by

$$|C^{As}_{4s}|^2 = a^{As}/3430 \qquad (11)$$

For $OV[S_2As(CH_3)_2]_2$, C^{As}_{4s} is 0.112 which is comparable to the value of C^{P}_{3s} (0.095) in the corresponding $OV[S_2P(CH_3)_2]_2$ complex. The small increase in coefficient in going from phosphorus to arsenic can probably be attributed to increased overlap between ligand σ and metal σ orbitals due to the larger size of the arsenic 4s orbital as compared to the phosphorus 3s orbital.

When pyridine displaces one of the sulfur atoms of the dimethyldithioarsinate ligand, the hyperfine interaction of the ^{75}As nucleus on this ligand disappears, and the interaction with the ^{75}As nucleus on the dimethyldithioarsinate chelate, which is not displaced, decreases. In species II, C^{As}_{4s} is 0.096 which is comparable to the value of C^{P}_{3s} (0.084) in the corresponding dithiophosphinate complex.[1] This decrease must reflect changes in the bonding at the vanadium atom when a pyridine nitrogen atom replaces a dimethyldithioarsinate sulfur atom from the equatorial coordination site.

Acknowledgment. This research was supported in part by the National Research Council of Canada under Operating Grant A5887. We gratefully acknowledge helpful discussions with Drs. R. G. Cavell and G. A. Miller.

Appendix

The determination of the mole fractions of the various vanadyl species in solutions of $OV[S_2As(CH_3)_2]_2$ containing Lewis bases and the magnetic parameters for each species was effected by manually digitizing the observed spectra at 200–500 points and fitting the digitized spectra with calculated spectra on a digital computer. An observed spectrum is thereby reduced to a set of n points $(B_i, \hat{S}_i)$ representing the observed intensity $\hat{S}_i$ of the first-derivative ESR signal at magnetic field B_i. The calculated intensity S_i at field B_i is determined by the values of the mole fractions of the various species and their magnetic parameters, which we denote collectively as $P_1, P_2, \ldots, P_m$ or $\{P_j\}$. The object of the computer fitting is to find the set of parameters $\{P_j\}$ which minimizes the sum of squared residuals $\sum_i(\hat{S}_i - S_i)^2$. We make the linearizing approximation that

$$S_i(P_1 + \Delta P_1, P_2 + \Delta P_2, \ldots, P_m + \Delta P_m) = S_i(P_1, P_2, \ldots, P_m) + \sum_j (\partial S_i/\partial P_j)\Delta P_j$$

and reduce the problem to determining the increments $\{\Delta P_j\}$ which correct the estimated parameters $\{P_j\}$ such that the sum of squared residuals is minimized. The derivatives $(\partial S_i/\partial P_j)$ depend on the values of the parameters $\{P_j\}$ so that the minimization procedure is an iterative one involving explicit evaluation of derivatives at each step. The increments $\{\Delta P_j\}$ for each iteration are determined by the method of steepest descents as described by Ralston.[20]

Registry No. I, 37448-72-9; II, 57885-73-1; III, 57919-11-6; $OV[S_2As(CH_3)_2]_2$·4py, 58023-81-7.

References and Notes

(1) G. A. Miller and R. E. D. McClung, *Inorg. Chem.*, **12**, 2552 (1973).
(2) M. Sato, Y. Fujita, and T. Kwan, *Bull. Chem. Soc. Jpn.*, **46**, 3007 (1973).
(3) M. Sato and T. Kwan, *Bull. Chem. Soc. Jpn.*, **46**, 3745 (1973).
(4) J. J. R. Frausto da Silva and R. Wootton, *Chem. Commun.*, 421 (1969); M. R. Caira, J. M. Haigh, and L. R. Nassimbeni, *J. Inorg. Nucl. Chem.*, **34**, 3171 (1972); M. R. Caira, J. M. Haigh, and L. R. Nassimbeni, *Inorg. Nucl. Chem. Lett.*, **8**, 109 (1972).
(5) J. Selbin, *Coord. Chem. Rev.*, **1**, 239 (1966).
(6) A. T. Casey, N. S. Ham, D. J. Mackey, and R. L. Martin, *Aust. J. Chem.*, **23**, 1117 (1970); M. Forster, H. Hertel, and W. Kuchen, *Angew. Chem.*, **82**, 842 (1970); A. Müller and P. Werle, *Chem. Ber.*, **104**, 3782 (1971); D. Johnstone, J. E. Fergusson, and W. T. Robinson, *Bull. Chem. Soc. Jpn.*, **45**, 3721 (1972).
(7) A. T. Casey, D. J. Mackey, and R. L. Martin, *Aust. J. Chem.*, **24**, 1587 (1971).
(8) W. Kuchen, M. Forster, H. Hertel, and B. Höhn, *Chem. Ber.*, **105**, 3310 (1972).
(9) B. J. McCormick, J. L. Featherstone, H. J. Stoklosa, and J. R. Wasson, *Inorg. Chem.*, **12**, 692 (1973).
(10) J. R. Wasson, G. M. Woltermann, and H. J. Stoklosa, *Fortschr. Chem. Forsch.*, **35**, 65 (1973).
(11) E. D. Day, Ph.D. Thesis, University of Alberta, 1972; R. G. Cavell, E. D. Day, W. Byers, and P. M. Watkins, *Inorg. Chem.*, **11**, 1591 (1972), and references therein.
(12) J. R. Wasson, *Inorg. Chem.*, **10**, 1531 (1971), and references therein.
(13) S. H. Glarum and H. J. Marshall, *J. Chem. Phys.*, **41**, 2182 (1964).
(14) R. A. Zingaro, K. J. Irgolic, D. H. O'Brien, and L. J. Edmonson, Jr., *J. Am. Chem. Soc.*, **93**, 5677 (1971).
(15) R. Wilson and D. Kivelson, *J. Chem. Phys.*, **44**, 154 (1966).
(16) The observed ESR spectra were digitized manually, and the spectral

parameters were refined using the least-squares criteria incorporated in the digital computer simulation program EPRLQ. Listings of this program and sample input data are available on request.
(17) E. DeBoer and E. L. Mackor, *Mol. Phys.*, **5**, 493 (1962).
(18) G. Miller, Ph.D. Thesis, University of Alberta, 1973.
(19) H. Hertel and W. Kuchen, *Chem. Ber.*, **104**, 1740 (1971).
(20) A. Ralston, "A First Course in Numerical Analysis", McGraw-Hill, New York, N.Y., 1965, pp 439–443.

Contribution from Welch Chemical Laboratories,
The University of Texas, Austin, Texas 78712

Organometallic Derivatives of the Transition Elements. I. Carbon-13 Nuclear Magnetic Resonance Studies of Bis(arene)chromium(0) Compounds

V. GRAVES and J. J. LAGOWSKI*

Received November 3, 1975 AIC50793S

The ^{13}C nuclear magnetic resonance spectra have been obtained for a series of bis(arene)chromium(0) compounds. The complexed arene is variously substituted by R, F, Cl, CF_3, NR_2, COOR. In monosubstituted bis(arene)chromium(0) complexes containing substituents which are known to perturb the resonance system of the arene, an analysis of the C-4 chemical shift indicates that in the bis(arene)chromium(0) complexes there is no transmission of substituent effects across the complexed ring. These results are interpreted to mean that a significant reduction of ring aromaticity occurs upon complexation to chromium, an effect attributed to the donation of arene π electron density into vacant metal orbitals. The reduction of ring aromaticity in the complexes explains the failure of the compounds to undergo electrophilic aromatic substitution. The availability of complexes with good leaving groups such as F and Cl, together with the reduced aromatic character of the ring, suggests nucleophilic aromatic substitution reactions on complexed rings may be feasible.

Introduction

Since Timms[1] first described the direct synthesis of bis(benzene)chromium(0) in 1969 from chromium metal atoms and benzene, a large number of bis(arene)chromium(0) complexes have been reported[2-6] (as well as tungsten and molybdenum analogues) in which substituents other than alkyl or aryl groups occur. The synthesis of these new compounds has refocused attention on the structure and chemistry of the arene–metal π complexes. One of the most perplexing and, to date, unanswered structural problems associated with these compounds is the degree of aromaticity in the ligand ring upon complexation to the metal atom. The classical structural criteria for resonance delocalization in the benzene molecule are coplanarity of the six carbon atoms and equivalent C–C bond lengths. Many of the early investigations of these compounds attempted to establish D_{6h} site symmetry for the ligand in bis(benzene)chromium(0). The x-ray work of Cotton[7] and a gas-phase electron diffraction study of bis(benzene)chromium(0) by Haaland[8] have provided conclusive experimental evidence for sixfold symmetry of the ligand.

Several semiempirical MO descriptions of the electronic structure of bis(benzene)chromium(0) are available in the literature.[9-16] In all of these treatments, the complexed ring is assumed to exhibit D_{6h} symmetry and the molecular energy levels predicted are compatible with a delocalized aromatic system but do not exclude the possibility of a reduction in aromaticity, provided that D_{6h} symmetry is maintained as the site symmetry for the ligand. Calculations place a −0.75 e charge on the ring, which is in approximate agreement with the experimentally estimated value of −0.55 e.[17] Experimentally, bis(benzene)chromium(0) exhibits zero dipole moment,[18] which does not necessarily imply the absence of a metal–ligand bond dipole but simply reflects the symmetrical nature of the molecule in which a net dipole cannot be detected.

The chemistry of the alkyl- and phenyl-substituted bis(arene)chromium(0) complexes prepared by the Fischer–Hafner method[19] appears to be severely limited. The attainable complexes do not undergo the usual electrophilic substitution reactions characteristic of an aromatic system.[20] Metalation occurs with amylsodium[21] and *N,N,N',N'*-tetramethylethylenediamine complexes of *n*-butyllithium.[22] The complexes also exhibit base-catalyzed hydrogen–deuterium exchange.[23,24] Nucleophilic substitution reactions have not been reported for the alkyl- and phenyl-substituted bis(arene)chromium(0) complexes which probably arise from the fact that these substituents are poor leaving groups. Semmelhack and Hall[25] have recently reported nucleophilic substitution reactions on chlorobenzene chromium tricarbonyl, emphasizing the electron-withdrawing character of the complexed $Cr(CO)_3$ moiety.

The bis(arene)chromium(0) complexes readily undergo a one-electron oxidation to form an air-stable, water-soluble cation. It is possible that the complexed arene rings do posses a delocalized electronic system but fail to undergo the usual electrophilic substitution reactions because the electrophiles in these reactions cause oxidation of the chromium complex before the desired reaction on the ligand can go to completion. On the other hand, an effective quenching of the aromaticity of the system upon complexation may also explain the failure of the usual electrophilic substitution reactions but would be virtually impossible to detect by chemical means due to the ease of complex oxidation.

Carbon-13 magnetic resonance spectroscopy appears to be a suitable method of estimating the π-electron density in the ligand, or at least of determining the extent of perturbation occurring in the resonance system when an aromatic hydrocarbon is complexed to a metal atom. Lauterbur[26] suggested that variations in the local π-electron densities primarily govern the ^{13}C shieldings in aromatic rings. A good correlation was established by Spiesecke and Schneider[27] between the carbon chemical shift and the local π-electron density.

The quantitative estimation of the electron density at specific carbon atoms in a chemical system is a tedious process. A considerably simpler and experimentally more accessible method of estimating changes in the π-electron density is based on the chemical shift of the carbon atom para to a substituent in a monosubstituted benzene. When substituent groups such as F, OCH_3, NR_2, are attached to a benzene nucleus, the full effect of the π-electron perturbation, relative to benzene, is reflected in the change in chemical shift observed for C-4. This effect has been verified by both empirical and theoretical